Fall 2020

Application of the "iDISCO" Full-Brain Tissue Clearing Method: A View of Dopamine and Inflammation in the HIV-1 Transgenic Rat

Kristin Nickole Kirchner

APPLICATION OF THE "iDISCO" FULL-BRAIN TISSUE CLEARING METHOD: A VIEW OF DOPAMINE AND INFLAMMATION IN THE HIV-1 TRANSGENIC RAT

by

Kristin Nickole Kirchner

Bachelor of Science
The University of South Carolina Upstate, 2017

Submitted in Partial Fulfillment of the Requirements

For the Degree of Master of Arts in

Experimental Psychology

College of Arts and Sciences

University of South Carolina

2020

Accepted by:

Steven Harrod, Director of Thesis

Rosemarie Booze, Reader

Charles Mactutus, Reader

Cheryl L. Addy, Vice Provost and Dean of the Graduate School

DEDICATION

I dedicate this thesis to my family: Karl, Andie, Joan, and Charles Kirchner, and Ann and Emory Hornsby. I would not be the person I am today without their sacrifices, guidance, and love. I thank them for always listening, no matter what I had to say. I thank my parents for giving me the gift of their knowledge, and I am proud to have been raised by them. This thesis is also dedicated to my dearest friends: Matthew, Austin, Emily, Colin, Chris, Kyle, Nolan, Josh, Josiah, Nick, Lee, Anah, and Rachel. From both near and far, their dedication to me has been unwavering throughout the years. I thank them sincerely for being the brightest parts of my days. I would also like to specially thank F.D.H. for his unconditional love.

ACKNOWLEDGEMENTS

I would like to acknowledge Dr. Steven Harrod, my primary mentor, and Dr. Rosemarie Booze, my secondary mentor for their guidance. I would also like to acknowledge Dr. Hailong Li and Dr. Charles Mactutus for their mentorship. Acknowledgement and thanks to fellow lab members Adam Denton, Jessica Illenberger, Dr. Kristen McLaurin, Victor Madormo, and Alex Steiner. This research was supported by National Institute of Health Grants NS100624, DA013137, HD043680, MH106392 and by a National Institute of Health T32 Training Grant 5T32GM081740.

ABSTRACT

The iDISCO (immunolabeling-enabled three-dimensional imaging of solvent-cleared organs) method is a quick, inexpensive, and easily adaptable tissue staining and clearing procedure that allows neuroscientists to study a protein of interest in a whole, unaltered tissue sample. While the iDISCO method was initially tested and validated for mice embryos and brains, the current experiment sought to adapt the method for use in the rat using HIV-1 transgenic (Tg) rat brain tissue. Antibodies for tyrosine hydroxylase and Iba-1 were validated in the HIV-1 Tg rat and in F344/N control rats using iDISCO. Confocal images were taken of tyrosine hydroxylase positive neurons in the substantia nigra area of male and female HIV-1 Tg and F344/N control rats. The HIV-1 Tg female rat was determined to have the most positive TH staining, followed by the control male, HIV-1 Tg male, and control female. Viewing the brain as a whole system rather than a series of individual pieces is the biggest advantage of the whole-brain tissue clearing iDISCO method.

TABLE OF CONTENTS

Dedication iii

Acknowledgements iv

Abstract v

List of Tables viii

List of Figures ix

List of Symbols x

List of Abbreviations xi

Chapter 1: Introduction 1

1.1 Tissue Clearing 1

1.2 HIV 4

Chapter 2: Materials and Methods 9

2.1 Ethics Statement 9

2.2 Subjects 9

2.3 Sample Preparation 9

2.4 Methanol Pretreatment 10

2.5 Immunolabeling 11

2.6 Clearing 11

2.7 Mounting 12

2.8 Imaging 12

2.9 Analysis 13

Chapter 3: Results 15

Chapter 4: Discussion 23

Chapter 5: Conclusions 27

References 28

Appendix A: Solution Recipes 38

Appendix B: Supplier Information 39

LIST OF TABLES

Table B.1 Supplier Information 39

LIST OF FIGURES

Figure 2.1 Representative Confocal Image.....14

Figure 3.1 Cleared Tissue.....16

Figure 3.2 Morphology of TH+ Neurons.....17

Figure 3.3 Morphology of Iba1 Positive Microglia.....18

Figure 3.4 TH+ Staining in HIV-1 Tg Female.....19

Figure 3.5 TH+ Staining in F344/N Male.....20

Figure 3.6 TH+ Staining in HIV-1 Tg Male.....21

Figure 3.7 TH+ Staining in F344/N Female.....22

LIST OF SYMBOLS

°C	Reference to specific temperature on the Celsius scale
µ	Unit prefix in the metric system denoting a factor of 10^{-6}
m	Unit prefix in the metric system denoting a factor of 10^{-3}

LIST OF ABBREVIATIONS

3DISCO..... 3D Imaging of Solvent-Cleared Organs

AAALAC..... Assessment and Accreditation of Laboratory Animal Care

cART..... Combination Antiretroviral Therapy

CCR5.....C-C Chemokine Receptor Type 5

DBE..... Dibenzyl Ether

DCM .....Dichloromethane

DMSO.....Dimethyl Sulfoxide

F344/N .....Fischer 344 rat

HIV .....Human Immunodeficiency Virus

IACUC.....Institutional Animal Care and Use Committee

Iba1 .....Ionized Calcium Binding Adaptor Molecule 1

iDISCO .....Immunolabeling-enabled Imaging of Solvent-clearing Organs

IHC..... Immunohistochemistry

L .....Liter

PBS ..... Phosphate-buffered Saline

PFA ..... Paraformaldehyde

RT ..... Room Temperature

Tg .....Transgenic

TH .....Tyrosine Hydroxylase

CHAPTER 1

INTRODUCTION

1.1 TISSUE CLEARING

Immunohistochemical (IHC) staining is a common procedure used to identify a target protein in a tissue sample. First implemented in the mid-1900s, and used continuously since, IHC uses antigen specific antibodies to mark proteins of interest (Coons et al., 1941; Ramos-Vara, 2005). Most IHC procedures follow a similar workflow. First, a tissue sample is fixed to preserve the tissue's morphology (Grizzle, 2009). After fixation, samples can easily be cut into thin sections using a vibratome, cryostat, or brain matrix. Most traditional IHC procedures call for a tissue width of between 10-100 µm (West, 2012). Tissue samples are then blocked for endogenous materials present in the sample. Peroxidase blocking prevents blood cells from interfering with later imaging, and serum blocking of endogenous antibodies is essential to prevent cross-reactivity with the secondary antibody. A primary antibody corresponding to the protein of interest is used, followed by a secondary antibody corresponding to the animal of origin of the primary antibody. The secondary antibody either fluoresces when in the presence of a specific wavelength of light or is compatible for use with a permanent dyeing protocol, such as the avidin-biotin complex method (Ramos-Vara & Miller, 2014). After mounting the sample, positive staining is viewed under a light or florescent microscope.

Traditional IHC protocol are generally uncomplicated, inexpensive, versatile, and are compatible with the powerful statistical procedure of stereology (West, 2012). The aim of most IHC experiments is to determine localization or quantification of a protein of interest. However, there are limitations to conventional free-floating or slide-based IHC that can make analysis using stereology difficult.

A tissue sample must meet strict criteria to be reliably assessed using stereology (West, 2012). First, conventional free-floating or slide-based IHC procedures involve dehydration steps and thus, tissues that start out appropriately thick may become too thin to be used in certain stereological probes. For tissue that is not homogenous, like the brain, dehydration-induced shrinkage of the sample may occur unevenly (Larsson, 1993). Second, traditional IHC protocols involve cutting the tissue samples into very thin (10-100 µm) slices, which can cause further loss of cells, structures, or proteins of interest. Because of this loss, the top and bottom of tissue samples are usually neglected in stereology, and thus, tissue is wasted (West, 2012). Third, important biological structures must be cut into many pieces to be compatible with traditional IHC protocol. Structures in pieces can no longer easily be analyzed as a whole, or as a component of a larger system. Finally, slide-based or free-floating protocols do not usually allow for deep penetration of the antibodies. Even if an antibody were able to penetrate a thicker sample, the sample would likely be too optically opaque to allow for the light penetration necessary for visualization on a microscope (Ariel, 2017).

Tissue clearing offers a solution to the aforementioned limitations of traditional IHC protocol. A sample that is transparent minimizes the scattering and absorption of light, which provides cellular level optical access to tissues that are intact (Rocha et al.,

2019; Richardson & Lichtman, 2015). Tissue clearing techniques turn a tissue transparent through delipidation, decolorization, and decalcification with the administration of solvents. Once the refractive index of the tissue sample matches the refractive index of the chosen imaging medium, the sample will appear completely transparent and can be properly imaged (Ueda et al., 2020).

Several tissue clearing techniques have been validated for use in the brain: hydrogel, hydrophilic, and hydrophobic. Hydrogel based techniques, such as CLARITY, secure biomolecules in the tissue by linking them to acryl-based hydrogels, which prevents structural damage and loss of proteins (Chung et al., 2013). However, hydrogel techniques utilize harsh chemicals that have the potential to damage more fragile tissues or antibodies, and denser tissue samples may not be compatible with some hydrogel protocol. Certain hydrogel techniques may also require expensive equipment or lead to tissue expansion. Hydrophilic techniques, like CUBIC and FocusClear, preserve 3D structure through the formation of hydrogen bonds within the tissue (Susaki, et al., 2014). Tissue expansion can also occur in certain hydrophilic protocol. The clearing ability of hydrogel and hydrophilic techniques often does not match that of hydrophobic methods, which is crucial for denser and thicker tissues (Ueda et al., 2020).

Immunolabeling-enabled three-dimensional imaging of solvent-cleared organs (iDISCO) is a hydrophobic clearing technique that improves upon previous hydrophobic techniques by eliminating the shrinkage that can occur (Renier et al., 2014). The iDISCO procedure removes water from the tissue in the initial dehydration step, thus reducing light scatter. Tissue is permeabilized during pretreatment to allow deep antibody penetration. Tissue that has undergone the iDISCO protocol is able to be handled easily

and can be imaged several times. If properly stored, tissues can still provide images for up to a year after initial processing. A hydrophobic technique such as iDISCO is relatively fast, does not require special equipment, and produces a sample that is easy to handle and store.

Originally, the iDISCO tissue clearing technique was described by Renier et al. (2014), who extended the utility of the 3DISCO procedure to include mice embryos and denser, adult organs of mice. The iDISCO technique has been implemented many times in mice, to great success (Renier et al, 2016; Silvestri et al., 2016). To date, however, the technique's full clearing ability has not been as well established in rats (Jing et al., 2018; Qi et al., 2019). Validation in the rat brain serves as an important advancement, as rats are used in approximately 50% of neuroscience publications and offer many advantages over mice due to their larger brain size and behavioral differences (Ellenbroek & Youn, 2016).

The first goal of the present experiment was to therefore demonstrate the full clearing ability of iDISCO in a commonly used species of laboratory rat, the F344/N Fischer rat. Because of their utility in neuroscience research, transgenic models of infectious diseases have been created in the species, such as the HIV-1 transgenic (Tg) rat.

1.2 HIV

The HIV-1 Tg rat was created on the F344/N background and provides researchers with a non-infectious animal model for HIV-1 (Reid et al., 2001). The HIV-1 provirus present in the transgenic rats has a functional deletion of two (*gag* and *pol*) of the three (*gag*, *pol*, and *env*) structural genes necessary for production of viral particles.

Despite these deletions, the genes of the provirus encoding for regulatory and accessory proteins, such as *tat*, remain functional. The HIV-1 Tg rat is a non-infectious model for HIV-1 induced viral protein exposure on brain function and overt behavior, which results in a model that is useful for studying the effect of viral proteins in the absence of active infection (Bertrand et al., 2018; Reid et al. 2001; Vigorito et al. 2015; McLaurin et al., 2018).

There are an estimated 37.9 million adults living with HIV, with 1.7 million new HIV infections occurring in 2018 alone (UNAIDS, 2019). To control the infection, individuals with the virus are often prescribed combination antiretroviral therapy (cART), a combination of fusion inhibitors, nucleotide and non-nucleotide reverse transcriptase inhibitors, integrase inhibitors, CCR5 antagonists, and protease inhibitors meant to suppress viral replication and block new infection (Bertrand et al., 2015; Sengupta & Siliciano, 2018). cART suppresses the virus's ability to replicate, which reduces the amount of circulating virus that is immune to treatment (Sengupta & Siliciano, 2018; Smyth et al., 2012). HIV-1 can enter a state of latency in some infected cells (Sengupta & Siliciano, 2018). Despite the suppression of replication from cART, latent HIV infection is still able to release HIV-1 neurotoxic proteins through astrocytes and microglia (Bertrand et al., 2015; Bertrand et al., 2014). Even transient exposure to these proteins may be enough to trigger a cascade of cellular events, such as apoptosis or inflammatory responses, that could lead to dendritic or synaptic loss (Aksenova et al., 2006; Bertrand et al., 2014).

Dysregulation of the dopaminergic system associated with HIV-1 has been well established in both human, clinical populations (Silvers et al., 2006; Gelman et al., 2006;

Kumar et al., 2011) and transgenic animal models (Lee et al., 2014; Javadi-Paydar et al., 2017; Bertrand et al., 2018). HIV-1 viral proteins Tat and gp120 have been theorized to directly affect the dopaminergic system, leading to behavioral and motivational alterations (Bennet et al., 1995; Fitting et al., 2015; Moran et al., 2012; Bertrand et al., 2018). Previous studies in the HIV-1 Tg rat have shown that dopaminergic impairment is greater in HIV-1 Tg animals when compared to controls; sex differences are also present, with HIV-1 Tg female rats being the most impaired group in both chemical and behavioral measures (Denton et al., 2019; McLaurin et al., 2017).

Tyrosine hydroxylase (TH) is the rate-limiting enzyme in the primary pathway of dopamine synthesis, and its detection is often used to draw conclusions about an organism's dopaminergic system. Decreased TH immunostaining in the striatum and substantia nigra areas indicate an enzymatic deficit in dopaminergic projections (Daubner et al., 2011). TH has previously been studied in the HIV-1 Tg rat using traditional IHC methodology (Goulding et al., 2019; Moran et al., 2012). At 8 months, male HIV-1 Tg rats were found to have significantly less TH+ staining when compared to controls; this same effect was not seen in younger (2-5 month old) rats (Goulding et al., 2019). In the present study, TH is used as an enzymatic marker for dopamine synthesis. It is hypothesized that HIV-1 Tg rats will show more TH impairment than controls, with HIV-1 Tg females showing the greatest impairment. The TH antibody used is rabbit polyclonal, and labels 62kDa, which corresponds to tyrosine hydroxylase (AB152, Millipore Sigma).

Microglia are a type of glial cell responsible for responding to cellular level threats that occur in the brain (Frank et al., 2019; Crotti et al., 2016). "Resting" microglia

sample the environment to look for threats with long, branching processes, while "activated" microglia will seek and destroy bacteria or foreign cells (Nimmerjahn et al., 2005). Microglia will activate in response to various stressors in the brain, such as physical trauma, seizure, or infections such as HIV-1 (Frank et al., 2019; Goulding et al., 2019; Rowson et al., 2016; Vera et al., 2016; Liu et al., 2018). Activation of microglia causes inflammation, which can induce a variety of behavioral, endocrine, and neural responses in multiple brain regions (Banks et al., 2015; Guillemin et al., 2004). Ionized calcium-binding adapter molecule 1 (Iba1) is a protein present in microglia that increases with activation (Ohsawa et al., 2004). Due to the interaction between the HIV-1 virus and microglia, and the effects of inflammation on the brain, microglia are an important target of study (Hauser & Knapp, 2015). The present study seeks to confirm the compatibility of an Iba1 antibody with the iDISCO clearing method for use in the HIV-1 Tg rat. The Iba1 antibody used is rabbit polyclonal, and was raised against a synthetic peptide corresponding to the Iba1 carboxy-terminal sequence (019-19741, FUJIFILM Wako).

The present experiment has three objectives. The first, and main, objective is to establish the validity of the iDISCO tissue clearing technique in F344/N and HIV-1 Tg rat brain tissue. The second objective is to validate two antibodies (TH and Iba1) for use in rat brain tissue. The third objective is to investigate the levels of TH+ staining in male and female HIV-1 Tg and F344/N control rats to more clearly understand the impact of HIV-1 associated viral protein exposure on dopamine production throughout the nigra-striatal and mesocorticolimbic dopamine systems. Using the iDISCO tissue clearing technique as a guide, TH and Iba1 antibodies were administered to male and female

F344/N control and HIV-1 Tg rat brains, with TH serving as a marker for dopamine production, and Iba1 marking for activated microglia.

CHAPTER 2

MATERIALS AND METHODS

2.1 ETHICS STATEMENT

The present research was conducted in accordance with the recommendations listed in the Guide for the Care and Use of Laboratory Animals from the National Institutes of Health. All rats used were housed in an AAALAC-accredited facility, with all procedures approved by the University of South Carolina Institutional Animal Care and Use Committee (IACUC).

2.2 SUBJECTS

One HIV-1 Tg female, one HIV-1 Tg male, one F344/N control female, and one F344/N control male were used for the present study. Dames to the subjects were obtained from Envigo (Indianapolis, IN). All rats were housed under conditions targeted to 21° ± 2 °C, 50% ±10% relative humidity with a 12 hour light-dark cycle. Subjects were housed with their littermates until the day of weaning.

2.3 SAMPLE PREPARATION

Ingredients for all solutions can be found in Appendix A. Supplier information for each chemical can be found in Appendix B. On the day of weaning (approximately postnatal day 21 to 24), a rat from a litter meeting proper transgene and sex criteria was selected for sacrifice. Rats were deeply anesthetized using sevoflurane. The rat was considered sufficiently anesthetized when it failed to respond to toe and tail pinch. In a fume hood, rats were laid supinely, and a lateral incision was made through the

abdominal wall beneath the rib cage to prepare for perfusion. A cut was made up through the bottom of the rib cage to the collarbone, cutting the diaphragm along the length of the rib cage. The left ventricle was pierced with a 23-gauge needle attached to a perfusion pump. After cutting open the right atrium, the perfusion began. Approximately 75mL of room temperature (RT) 100mM (1X) phosphate buffered saline (PBS) was used to flush the vasculature. The transcardial perfusion was continued with approximately 100mL of 4% paraformaldehyde (PFA) buffered in 1X PBS. Once the rat was fully perfused, the brain was removed from the skull. Meninges were removed. Each brain was sliced sagittally using a razor blade into sections approximately 3mm in width. Each section was fixed in 4% PFA in 1X PBS in a sealed, 5mL plastic tube overnight at 4° C on a shaker. All steps were performed in fully filled, closed tubes to avoid oxidation of the samples. The next day, sections continued to fix at RT on a shaker for 1 additional hour. Sections were placed in a new 5mL tube and were washed 3 times with 1X PBS at RT for 30 minutes.

2.4 METHANOL PRETREATMENT

Samples were incubated in increasing concentrations of methanol for 1 hour per concentration at RT. The concentrations used were 20% methanol/80% deionized water, 40% methanol, 60% methanol, 80% methanol, and 100% methanol twice. Each sample was then chilled in fresh 100% methanol at 4° C for approximately 10 minutes. Samples were then incubated overnight in a 66% dicholoromethane/33% methanol solution at RT with shaking. Each sample was washed with methanol at RT for 30 minutes, twice. Samples were then chilled in 100% methanol at 4° C for approximately 10 minutes. Samples were bleached in chilled, freshly prepared 5% hydrogen peroxide/95% methanol

overnight at 4° C. Samples were then rehydrated in decreasing concentrations of methanol for 1 hour per concentration at RT. The concentration order used was 80% methanol/20% deionized water, 60% methanol, 40% methanol, 20% methanol, followed by a 1 hour incubation of 1X PBS. Samples were washed in PTx.2 for 1 hour at RT, twice.

2.5 IMMUNOLABELING

Samples were incubated in permeabilizing solution for 2 days at 37°C in a closed, incubator water bath. After removal from the permeabilizing solution, samples were incubated in blocking solution for 2 days at 37°C in a closed, incubator water bath. After 2 days, one hemisphere from each animal was incubated with the tyrosine hydroxylase (TH) primary antibody at a concentration of 1:100 (AB152, Millipore Sigma) in 92% PTwH/5% DMSO/3% goat serum for 7 days at 37°C in a closed, incubator water bath. The other hemisphere was incubated with the Iba1 primary antibody (019-19741, FUJIFILM Wako) at a concentration of 1:200 in the same solution and conditions. After 7 days, samples were washed in PTwH 5 times at 1 hour per wash, and then stored in PTwH at RT overnight. The next day, samples were incubated in Alexa Fluor Plus 647 (A32733, Invitrogen) secondary antibody in 97% PTwH/3% goat serum for 7 days at 37°C in a closed, incubator water bath. Goat serum was used because it corresponded with the secondary antibody chosen for labelling. Samples were washed in PTwH 5 times at 1 hour per wash, and then stored in PTwH at RT overnight.

2.6 CLEARING

Samples were incubated in increasing concentrations of methanol for 1 hour per concentration at RT. The concentrations used were 20% methanol/80% deionized water,

40% methanol, 60% methanol, 80% methanol, and 100% methanol. The samples were then incubated overnight in fresh 100% methanol at RT. After this, samples were incubated in 66% DCM/33% methanol for 3 hours, with shaking, at RT. Samples were then placed in DBE and left in a dark place at RT until ready for mounting. Samples were mounted after they were clear.

2.7 MOUNTING

3D printed chambers were ordered using the 3D models found on the idisco.info website. Chambers were printed using Visijet M3 Crystal resin, as it is will not degrade in the presence of DBE. Chambers with a depth of 3mm were used. Chambers were secured to microscope slides using Kwik-sil epoxy (VWR), which cures in the presence of DBE. This epoxy also does not form a permanent bond to the chamber, so samples are able to be remounted and reimaged. Samples were placed in the space within the chamber, and the chamber was filled with DBE. A 0.17 mm coverslip was placed over the chamber, and light pressure was applied to the slide to flatten the sample and form a seal with the chamber. While still applying pressure, the edges of the coverslip were sealed with Kwik-sil epoxy. Pressure was applied for 5 minutes until the epoxy cured. After curing, the chamber was rotated to allow air bubbles to escape from the filling inlet. Additional DBE was added into the chamber via a syringe to ensure that the sample was not exposed to air. The filling inlet was sealed with epoxy.

2.8 IMAGING

Images were obtained using a Nikon TE-2000E confocal microscope (Nikon, Tokyo, Japan) running Nikon's EZ-C1 software (version 3.81b). Tyrosine hydroxylase excitation was achieved utilizing a HeNe laser set to emit at 632 nm. The detector was set

to 650 nm. Images were obtained at 4x and 10x magnification, using the medium and large pinhole sizes provided by the EZ-C1 software. The 650LP gain for all images was set to 7.50 B. The substantia nigra, nucleus accumbens, prefrontal cortex, and ventral tegmental areas were identified and imaged in each rat when possible. Approximately 20 images were obtained per animal.

2.9 ANALYSIS

Out of the approximately 20 images obtained for each animal, the 4 images per animal which displayed the most positive fluorescence were chosen. Each animal was ranked from greatest to least TH expression. The ranking was first established by the primary researcher, but to avoid potential bias, three other researchers who were blind to condition were given criteria for positive staining and were also allowed to rank the overall TH expression of each animal. Four representative images were obtained for each animal used. Figure 2.1 shows a representative confocal image for TH in the substantia nigra region shown to all other raters. Raters blind to condition were shown this image, along with the description that marker “A” represents dense, positive staining, marker “B” represents sparse positive staining, and marker “C” represents tissue that is not positively stained. Raters were instructed to consider the overall staining present in the 4 images.

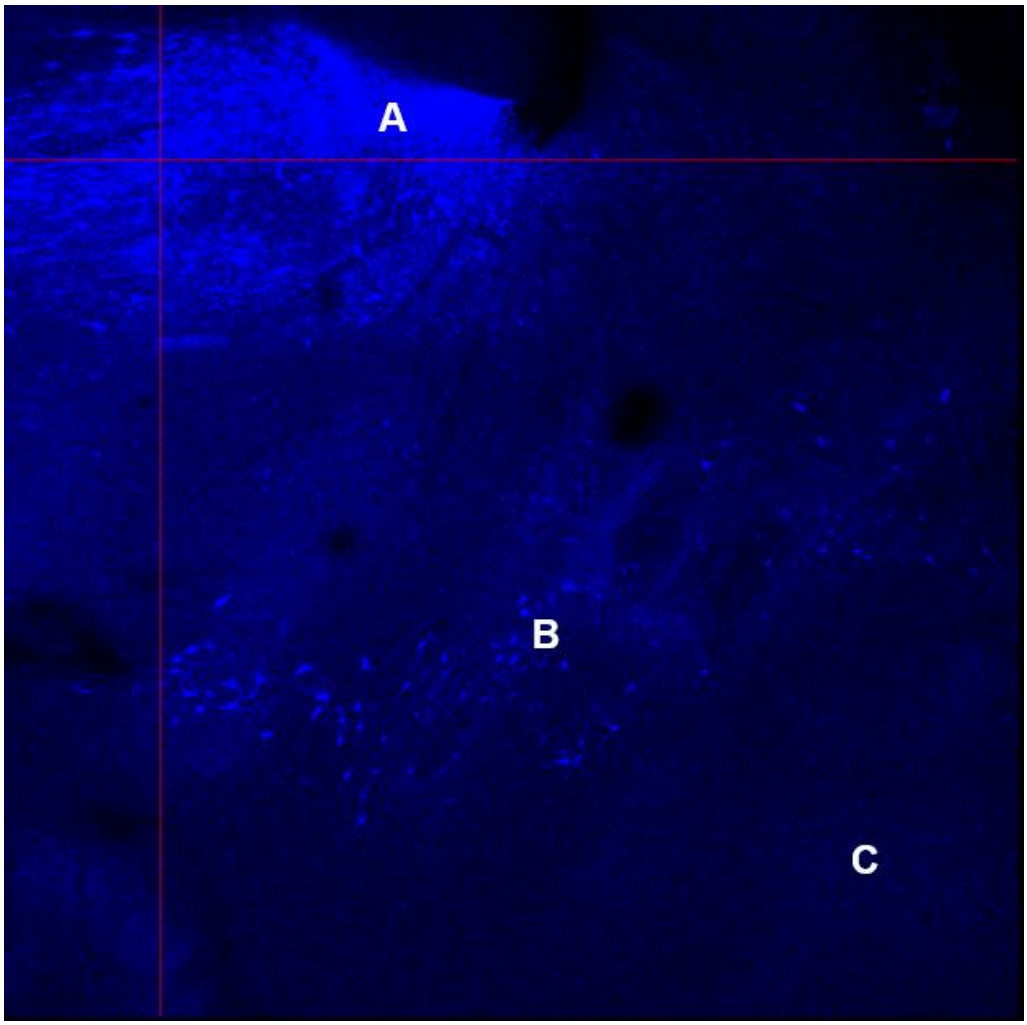

Figure 2.1: A representative confocal image from the HIV-1 Tg female (4x magnification). “A” represents dense TH staining, “B” sparse TH staining, and “C” no TH staining.

CHAPTER 3

RESULTS

F344/N and HIV-1 Tg rat brain tissues were able to be fully cleared by the present study's adjusted tissue clearing protocol (Figure 3.1). Increasing the length of the antibody incubation time allowed the antibody to fully penetrate the thick tissue. Changing the blocking serum to correspond according to the primary antibody reduced background staining. There was no noticeable difference in clearing between HIV-1 Tg tissue and F344/N control tissue.

TH and Iba1 staining were both compatible with the tissue clearing method used and had no noticeable detrimental interactions with the HIV-1 provirus. Figure 3.2 shows typical morphology of a TH positive neuron, with a large soma and several branching processes (Roostalu et al., 2019). Figure 3.3 shows Iba1 stained activated microglia, which have small cell bodies and shorter extending processes (Ransohoff & Cardona, 2010). Because the expected cell morphology was observed, the antibodies were considered to be successful in staining and compatible with the protocol.

Four representative images were chosen for each animal used. Blinded rankings were in 100% agreeance with the non-blinded ranking. The order of most to least TH+ staining was determined to be as follows: HIV-1 Tg female (Figure 3.4), F344/N control male (Figure 3.5), HIV-1 Tg male (Figure 3.6), F344/N control female (Figure 3.7).

Figure 3.1: A cleared brain tissue sample in DBE.

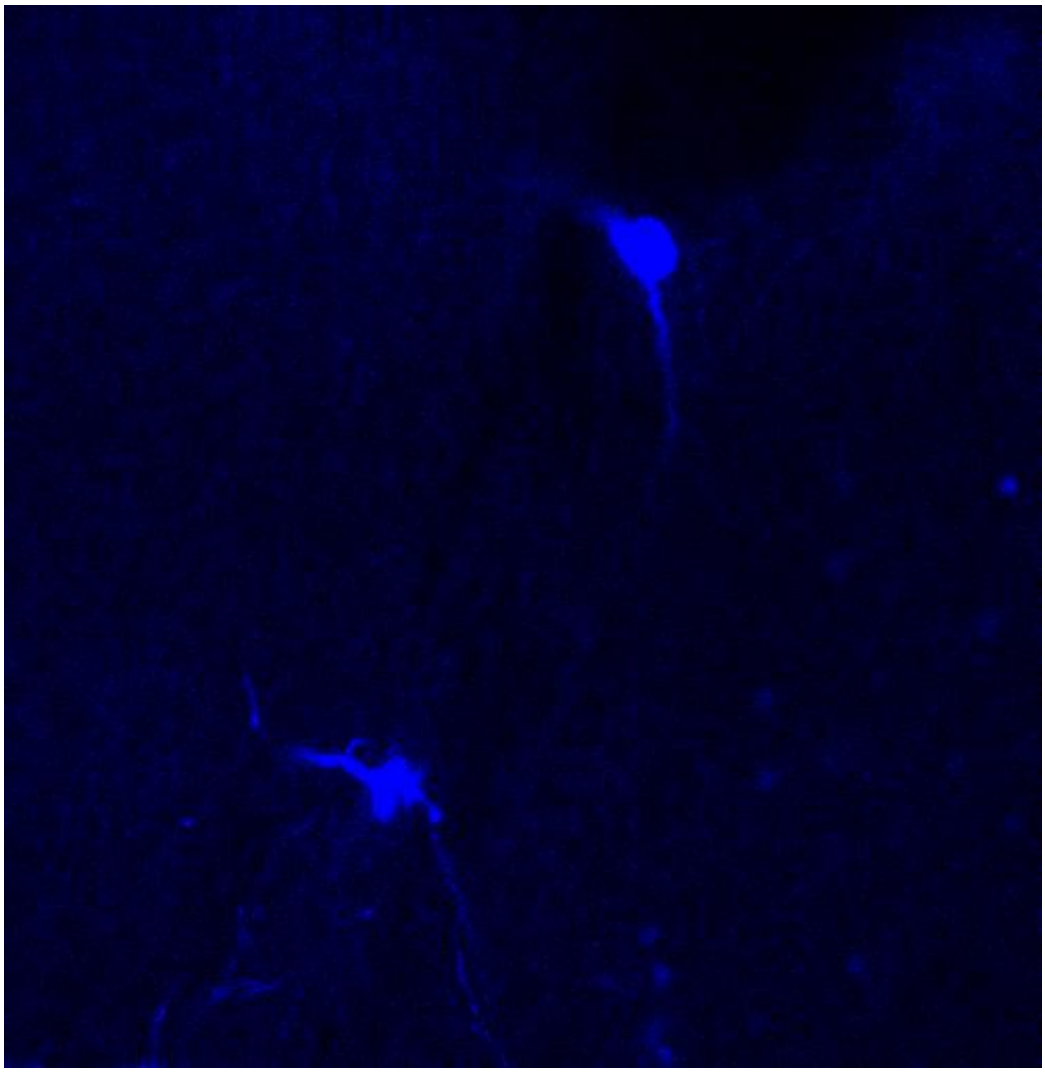

Figure 3.2: TH positive neurons (20x magnification, F344/N control male).

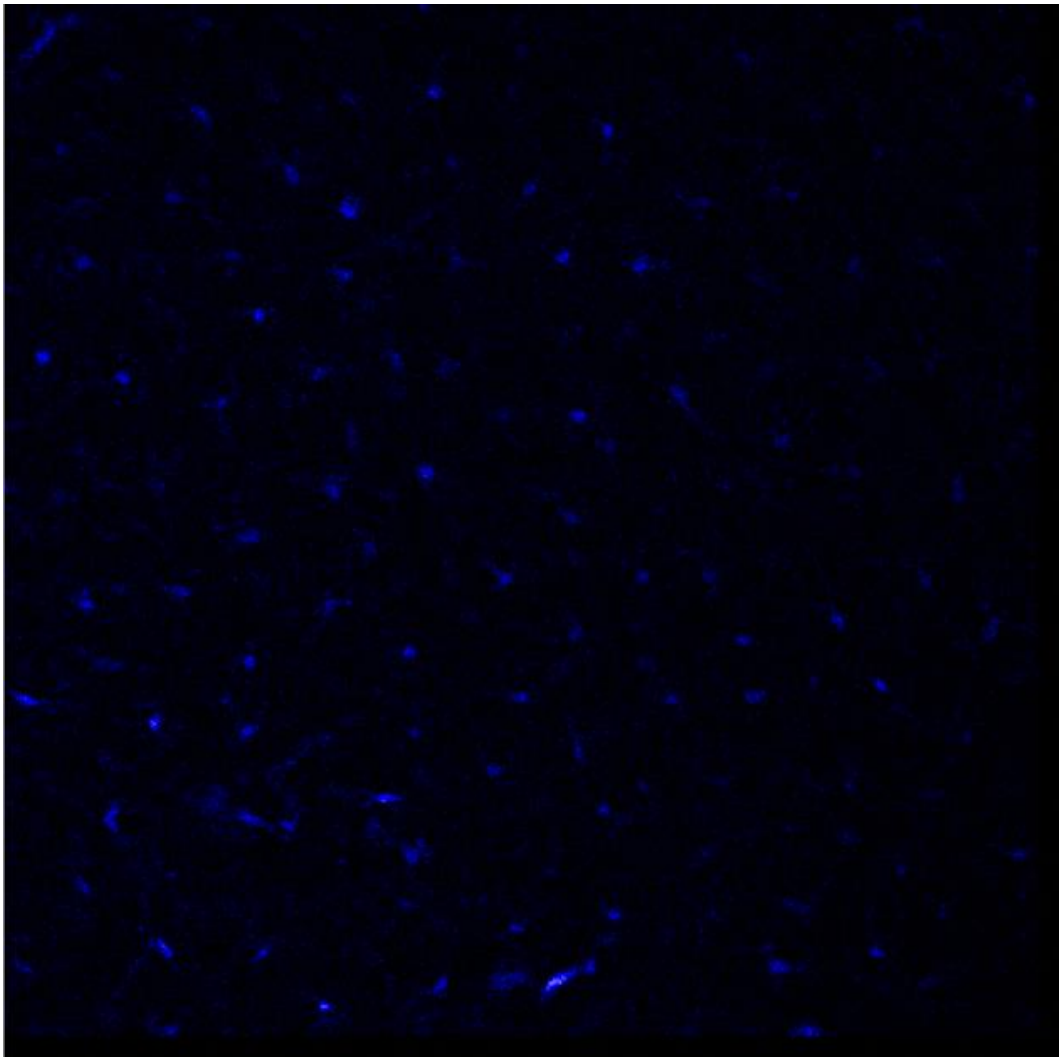

Figure 3.3: Iba1 positive microglia (20x magnification, F344/N control male).

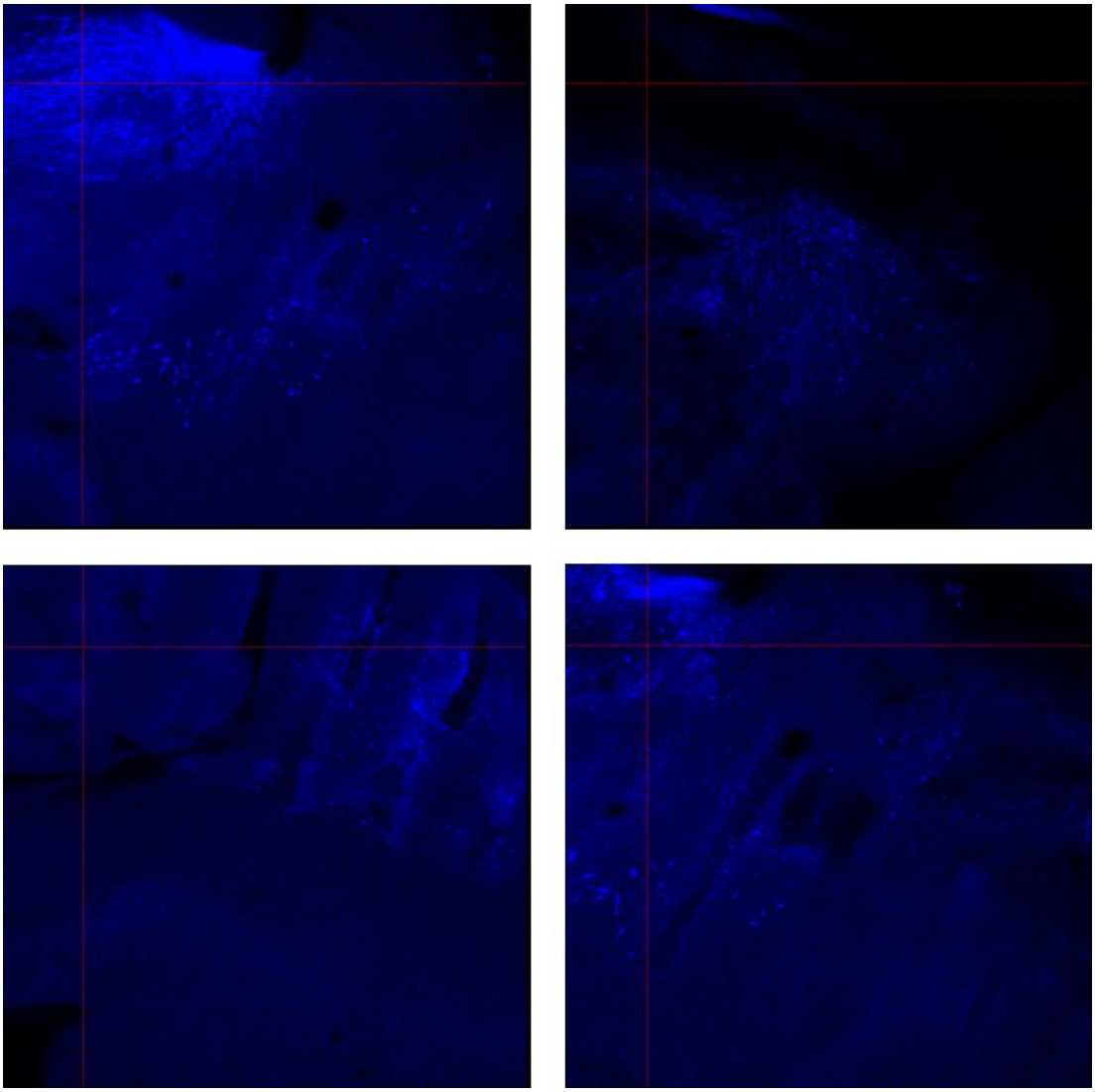

Figure 3.4: Four representative images of TH+ staining in the HIV-1 Tg female (4x magnification).

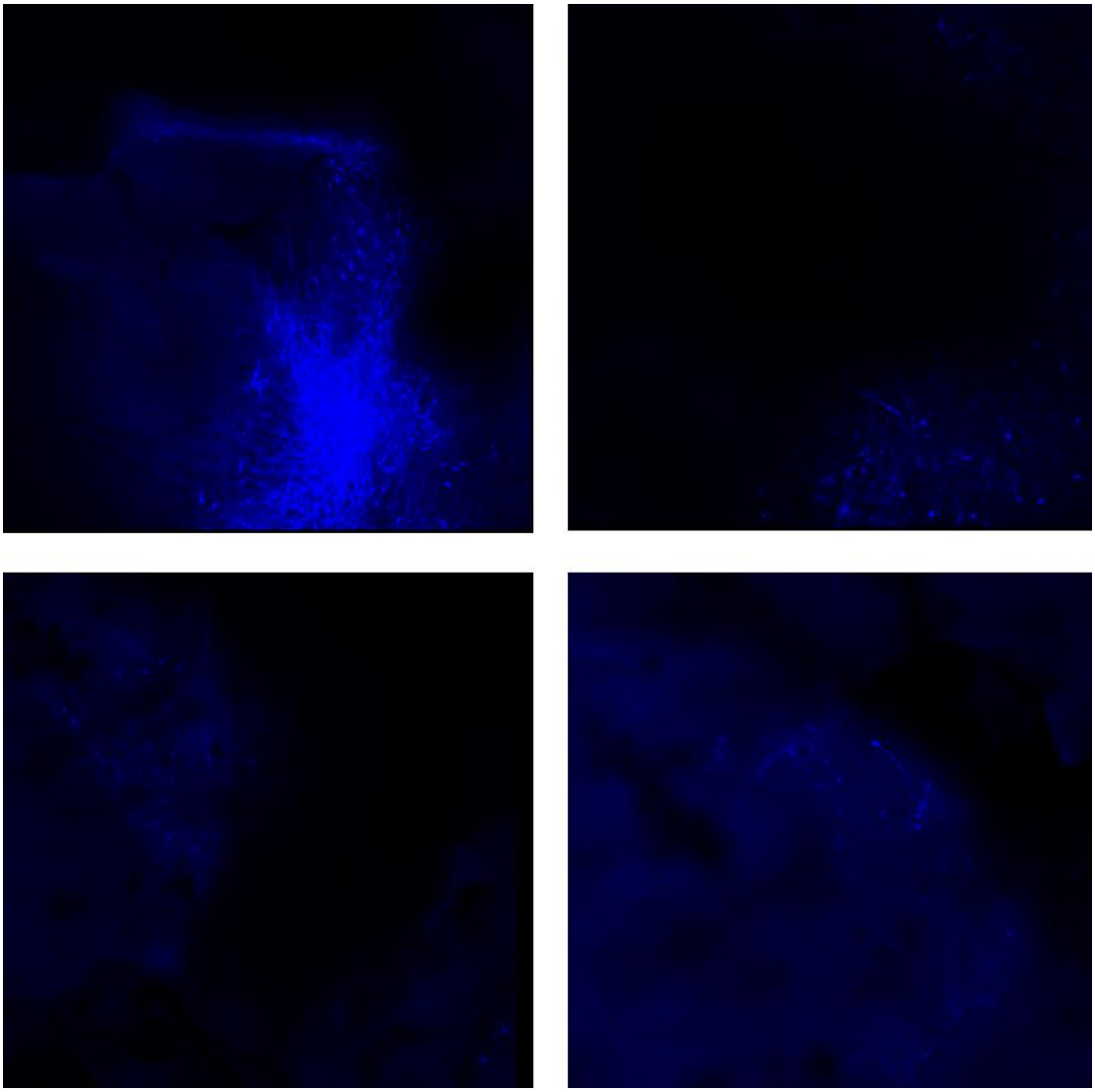

Figure 3.5: Four representative images of TH+ staining in the F344/N male (4x magnification).

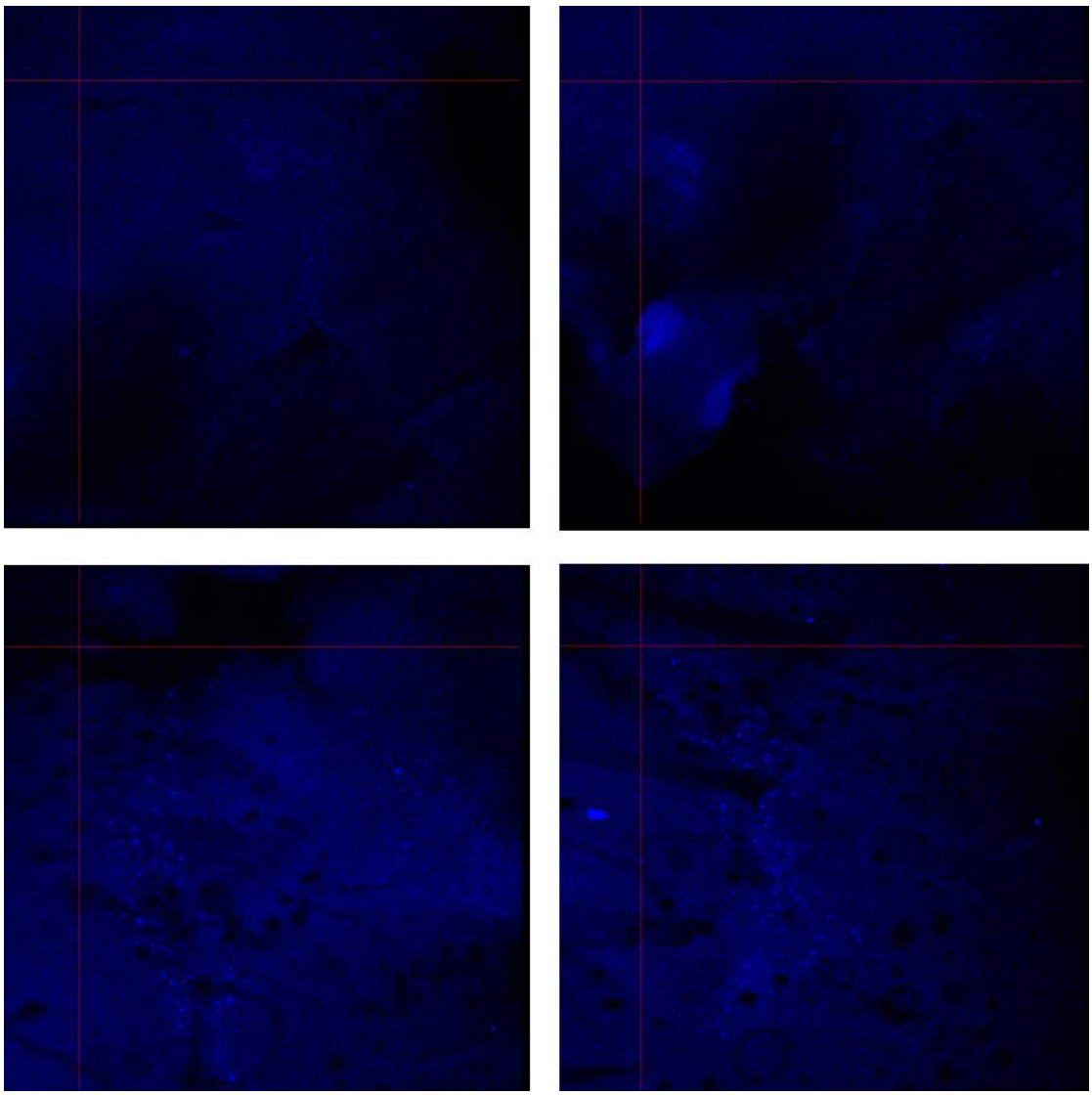

Figure 3.6: Four representative images of TH+ staining in the HIV-1 Tg male (4x magnification).

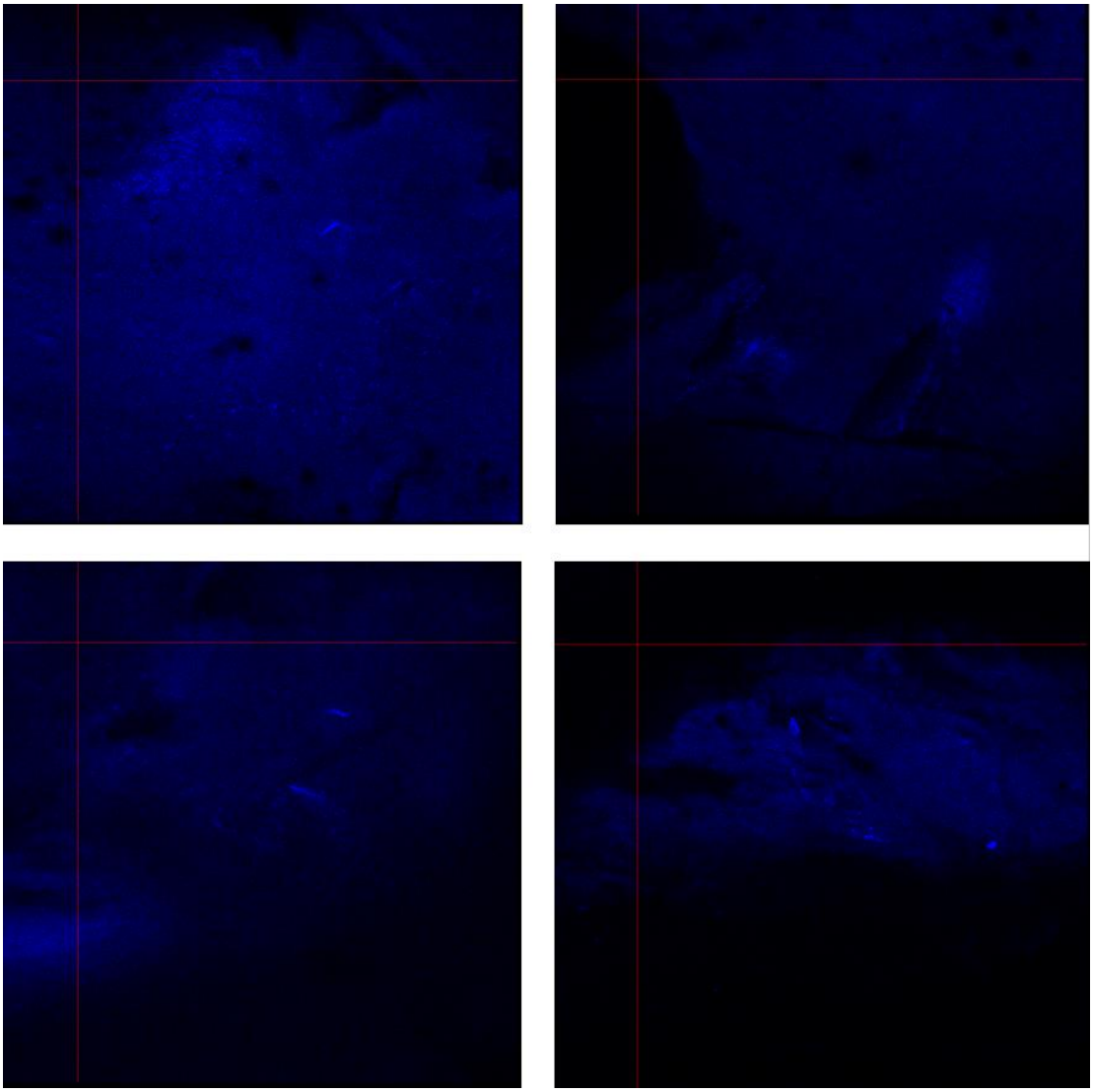

Figure 3.7: Four representative images of TH+ staining in the F344/N female (4x magnification).

CHAPTER 4

DISCUSSION

The immunostaining findings from the present study partially supported the original hypothesis. HIV-1 Tg females were determined to have the most TH+ staining, followed by F344/N males, HIV-1 Tg males, and F344/N females. Previous research has shown that TH staining in the substantia nigra is reduced in HIV-1 Tg male rats, with more TH loss seen over time (Webb et al., 2010; Goulding et al., 2019). This finding is also present in male-dominated studies of adult HIV-1 infected human brain tissue (Gelman et al., 2006). In the present study, this same effect was also seen, with the F344/N control male rat showing more TH positive staining when compared to the HIV-1 Tg male.

When compared to their male counterparts, HIV-1 Tg females present delayed task acquisition, less accurate signal detection, decreased dopamine release, impaired temporal processing, and decreased locomotor activity (McLaurin et al., 2017; Denton et al., 2019). Estrogen and phytoestrogens have been shown to prevent neuronal damage caused by Tat, reverse F-actin loss, and reduce HIV-1 associated motor and cognitive dysfunction (Adams et al. 2010; Bertrand et al. 2015; Wallace et al. 2006). Sex differences have also been observed in human clinical populations, where HIV-1 positive women have been shown to have higher levels of neurocognitive impairment than HIV-1 positive men (Royal et al., 2016; Sundermann et al., 2019). Based on this prior research, it was expected that the traditionally impaired HIV-1 Tg females would also have the

lowest overall TH levels. This was not the case, as the HIV-1 Tg female was determined to have the most positive TH staining out of the four animals tested. The current data suggest the presence of a sex by genotype interaction in relation to TH.

TH is traditionally used as an indicator of dopamine production. However, it is not entirely correct to make the assumption that more TH always indicates more dopamine production. TH is the rate-limiting enzyme that catalyzes the hydroxylation of tyrosine to L-DOPA, which can then be converted to dopamine using aromatic amino acid decarboxylase (Flatmark, 2000). TH is activated when the amount of neurotransmitter required increases at a catecholaminergic synapse, and activation is sustained until the requirement is lessened. TH is inactivated via feedback inhibition from the catecholamine neurotransmitters it helps create (Daubner et al., 2011). Previous research has shown that TH concentration and activation can even be increased following the destruction of catecholaminergic terminals, as if to compensate for the loss (Zigmond et al., 1984; Acheson et al., 1981). The increased TH levels seen in the female HIV-1 rat of the present study are possibly part of the compensatory action of TH in response to lowered dopamine in the system (Iuvone, 1983). Metabolite level differences have been previously been observed in HIV-1 positive patients when compared to controls (Ghannoum et al., 2013). With this in mind, an important consideration is the role that the HIV-1 virus might have in affecting other chemicals in the chain of dopamine synthesis such as L-DOPA, DOPA decarboxylase, or phenylalanine hydroxylase.

The present data have several severe limitations. Firstly, it cannot be ignored that each sex and genotype was represented by only one subject, which opens up the possibility that a non-representative subject happened to be randomly chosen. Thus,

while preliminary differences exist in this small sample size, a larger sample is necessary to confirm the present observed differences. The data presented here are observational in nature, and are not backed by any quantitative analysis. Quantitative analyses are limited by the tools currently available for the rat brain. Currently, investigative tools such as ClearMap exist to analyze cleared tissue of the mouse brain, but 3D rat brain atlases are still in development (Renier et al., 2016; Branch et al., 2019).

For the present study, rats were processed on the day of weaning (approximately day 21 of life). While it is not proper to make a direct comparison between rat age and the corresponding age of a human, a rat of weaning age is closer developmentally to a pre-pubescent human than to an adult (Sengupta, 2013). Rats do not reach sexual maturity until approximately 7 weeks of age, which means that female rats at weaning have not yet established their estrous cycles (Blunn, 1939). It is possible that female HIV-1 Tg rats have more TH than control females before sexual maturity, but more research would be needed to consider this possibility. As women account for roughly half of human HIV-1 cases, and sex differences are consistently observed in HIV-1 Tg rats, sex effects and interactions should continue to be investigated down to the molecular level (UNAIDS, 2019).

The tissue clearing results from the present study exhibited that the hydrophobic iDISCO clearing method is viable in large sections of both F344/N control and HIV-1 Tg rat brain tissue. The present protocol differs in a few important ways from the original by Renier, et al. (2014). Firstly, overall reduction of background staining was achieved by specifying the blocking serum used in the blocking, primary, and secondary antibody steps. Clearer images, reduced background signal, and more accurate staining was

achieved by using the serum corresponding to the secondary antibody (in this case, goat), instead of the donkey serum used in the original iDISCO protocol. Incubation time across the protocol was increased to account for larger tissue size and differing tissue density, which allowed for complete antibody penetration. TH and Iba1 antibodies were both validated for use with this method and in F344/N control and HIV-1 Tg rat brain tissue.

There are a few important considerations and limitations to the present tissue-clearing protocol. Despite the desire to leave the brain tissue intact, cutting the tissue to a smaller size is necessary due to the current physical limitations of the iDISCO imaging chambers. Maximum tissue thickness is also limited by the physical limitations of the confocal microscope; chambers that exceed a certain vertical height will collide with the lenses of the confocal microscope, and extremely thick tissues may not be able to be properly focused. While tissue clearing provides the advantage of imaging thicker tissue sections, it does truly leave the tissue sections clear, and thus, devoid of many natural landmarks.

CHAPTER 5

CONCLUSIONS AND FUTURE DIRECTIONS

Overall, the iDISCO technique is an extremely versatile, easy to implement, and low cost procedure with a growing list of validated antibodies. The present study provides continued evidence that the iDISCO tissue clearing technique is viable in brain tissues of the rat, has no discernible detrimental interactions with HIV-1 viral proteins, and is compatible with TH and Iba1 antibodies. Now, new investigative research questions can be explored utilizing this tissue clearing technique.

REFERENCES

Acheson, A. L., & Zigmond, M. J. (1981). Short and long term changes in tyrosine hydroxylase activity in rat brain after subtotal destruction of central noradrenergic neurons. *The Journal of neuroscience : the official journal of the Society for Neuroscience*, *1*(5), 493–504. https://doi.org/10.1523/JNEUROSCI.01-05-00493.1981

Adams, S. M., Aksenova, M. V., Aksenov, M. Y., Mactutus, C. F., & Booze, R. M. (2010). ER-β mediates 17β-estradiol attenuation of HIV-1 Tat-induced apoptotic signaling. *Synapse*, *64*(11), 829-838.

Aksenova, M. V., Silvers, J. M., Aksenov, M. Y., Nath, A., Ray, P. D., Mactutus, C. F., & Booze, R. M. (2006). HIV-1 Tat neurotoxicity in primary cultures of rat midbrain fetal neurons: changes in dopamine transporter binding and immunoreactivity. *Neuroscience letters*, *395*(3), 235-239.

Ariel P. (2017). A beginner's guide to tissue clearing. *The international journal of biochemistry & cell biology*, *84*, 35–39. https://doi.org/10.1016/j.biocel.2016.12.009

Banks, W. A., Gray, A. M., Erickson, M. A., Salameh, T. S., Damodarasamy, M., Sheibani, N., Meabon, J. A., Wing, E. E., Morofuji, Y., Cook, D. G., & Reed, M. J. (2015). Lipopolysaccharide-induced blood-brain barrier disruption: roles of cyclooxygenase, oxidative stress, neuroinflammation, and elements of the neurovascular unit. *Journal of neuroinflammation*, *12*(1), 223.

Bennett, B. A., Rusyniak, D. E., & Hollingsworth, C. K. (1995). HIV-1 gp120-induced neurotoxicity to midbrain dopamine cultures. *Brain research, 705*(1-2), 168-176.

Bertrand, S. J., Mactutus, C. F., Aksenova, M. V., Espensen-Sturges, T. D., & Booze, R. M. (2014). Synaptodendritic recovery following HIV Tat exposure: neurorestoration by phytoestrogens. *Journal of neurochemistry*, *128*(1), 140-151.

Bertrand, S. J., Mactutus, C. F., Harrod, S. B., Moran, L. M., & Booze, R. M. (2018). HIV-1 proteins dysregulate motivational processes and dopamine circuitry. *Scientific reports*, *8*(1), 1-17.

Bertrand, S., Hu, C., Aksenova, M., Mactutus, C., & Booze, R. (2015). HIV-1 Tat and cocaine mediated synaptopathy in cortical and midbrain neurons is prevented by the isoflavone Equol. *Frontiers in microbiology*, *6*, 894.

Blunn, C. T. (1939). The age of rats at sexual maturity as determined by their genetic constitution. *The Anatomical Record*, *74*(2), 199-213.

Branch, A., Tward, D., Vogelstein, J. T., Wu, Z., & Gallagher, M. (2019). An optimized protocol for iDISCO+ rat brain clearing, imaging, and analysis. *bioRxiv*, 639674.

Chung, K, Wallace, J, Kim, S et al. (2013). Structural and molecular interrogation of intact biological systems. *Nature, 497*, 332–337.

Coons, A. H., Creech, H. J., & Jones, R. N. (1941). Immunological properties of an antibody containing a fluorescent group. *Proceedings of the society for experimental biology and medicine*, *47*(2), 200-202.

Crotti, A., & Ransohoff, R. M. (2016). Microglial physiology and pathophysiology: insights from genome-wide transcriptional profiling. *Immunity*, *44*(3), 505-515.

Daubner, S. C., Le, T., & Wang, S. (2011). Tyrosine hydroxylase and regulation of dopamine synthesis. *Archives of biochemistry and biophysics*, *508*(1), 1–12. https://doi.org/10.1016/j.abb.2010.12.017

Denton, A. R., Samaranayake, S. A., Kirchner, K. N., Roscoe, R. F., Berger, S. N., Harrod, S. B., Mactutus, C. F., Hashemi, P., & Booze, R. M. (2019). Selective monoaminergic and histaminergic circuit dysregulation following long-term HIV-1 protein exposure. *Journal of neurovirology*, *25*(4), 540-550.

Ellenbroek, B., & Youn, J. (2016). Rodent models in neuroscience research: is it a rat race?. *Disease models & mechanisms*, *9*(10), 1079–1087. https://doi.org/10.1242/dmm.026120

Fitting, S., Booze, R. M., & Mactutus, C. F. (2015). HIV-1 proteins, Tat and gp120, target the developing dopamine system. *Current HIV research*, *13*(1), 21–42. https://doi.org/10.2174/1570162x13666150121110731

Flatmark, T. (2000). Catecholamine biosynthesis and physiological regulation in neuroendocrine cells. *Acta physiologica scandinavica*, *168*(1), 1-18.

Frank, M. G., Fonken, L. K., Watkins, L. R., & Maier, S. F. (2019, October). Microglia: Neuroimmune-sensors of stress. In *Seminars in cell & developmental biology* (Vol. 94, pp. 176-185). Academic Press.

Gelman, B. B., Spencer, J. A., Holzer, C. E., & Soukup, V. M. (2006). Abnormal striatal dopaminergic synapses in National NeuroAIDS Tissue Consortium subjects with HIV encephalitis. *Journal of Neuroimmune Pharmacology*, *1*(4), 410-420.

Ghannoum, M. A., Mukherjee, P. K., Jurevic, R. J., Retuerto, M., Brown, R. E., Sikaroodi, M., Webster-Cyriaque, J., & Gillevet, P. M. (2013). Metabolomics

reveals differential levels of oral metabolites in HIV-infected patients: toward novel diagnostic targets. *Omics: a journal of integrative biology*, *17*(1), 5–15. https://doi.org/10.1089/omi.2011.0035

Goulding, D. R., Kraft, A., Mouton, P. R., McPherson, C. A., Avdoshina, V., Mocchetti, I., & Harry, G. J. (2019). Age-Related Decrease in Tyrosine Hydroxylase Immunoreactivity in the Substantia Nigra and Region-Specific Changes in Microglia Morphology in HIV-1 Tg Rats. *Neurotoxicity research*, *36*(3), 563-582.

Grizzle W. E. (2009). Special symposium: fixation and tissue processing models. *Biotechnic & histochemistry: official publication of the Biological Stain Commission*, *84*(5), 185–193. https://doi.org/10.3109/10520290903039052

Guillemin, G. J., & Brew, B. J. (2004). Microglia, macrophages, perivascular macrophages, and pericytes: a review of function and identification. *Journal of leukocyte biology*, *75*(3), 388-397.

Hauser, K. F., & Knapp, P. E. (2014). Interactions of HIV and drugs of abuse: the importance of glia, neural progenitors, and host genetic factors. *International review of neurobiology*, *118*, 231–313. https://doi.org/10.1016/B978-0-12-801284-0.00009-9

Iuvone, P. M. (1983). Short-term regulation of tyrosine hydroxylase in tonically-active and in tonically-inactive dopamine neurons: Effects of haloperidol and protein phosphorylation. *Life sciences*, *33*(13), 1315-1324.

Javadi-Paydar, M., Roscoe, R. F., Jr, Denton, A. R., Mactutus, C. F., & Booze, R. M. (2017). HIV-1 and cocaine disrupt dopamine reuptake and medium spiny neurons

in female rat striatum. *PloS one*, *12*(11), e0188404. https://doi.org/10.1371/journal.pone.0188404

Jing, D., Zhang, S., Luo, W., Gao, X., Men, Y., Ma, C., ... & Zhao, Z. (2018). Tissue clearing of both hard and soft tissue organs with the PEGASOS method. *Cell research*, *28*(8), 803-818.

Kumar, A. M., Ownby, R. L., Waldrop-Valverde, D., Fernandez, B., & Kumar, M. (2011). Human immunodeficiency virus infection in the CNS and decreased dopamine availability: relationship with neuropsychological performance. *Journal of neurovirology*, *17*(1), 26-40.

Larsson, L. I. (1993). Tissue preparation methods for light microscopic immunohistochemistry. *Applied Immunohistochemistry*, *1*(1), 2-16.

Lee, D. E., Reid, W. C., Ibrahim, W. G., Peterson, K. L., Lentz, M. R., Maric, D., Choyke, P. L., Jagoda, E. M., & Hammoud, D. A. (2014). Imaging dopaminergic dysfunction as a surrogate marker of neuropathology in a small-animal model of HIV. *Molecular imaging*, *13*, 10.2310/7290.2014.00031. https://doi.org/10.2310/7290.2014.00031

Liu, J., Xu, E., Tu, G., Liu, H., Luo, J., & Xiong, H. (2017). Methamphetamine potentiates HIV-1gp120-induced microglial neurotoxic activity by enhancing microglial outward K^+ current. *Molecular and cellular neurosciences*, *82*, 167–175. https://doi.org/10.1016/j.mcn.2017.05.009

McLaurin, K. A., Booze, R. M., Mactutus, C. F., & Fairchild, A. J. (2017). Sex matters: robust sex differences in signal detection in the HIV-1 transgenic rat. *Frontiers in behavioral neuroscience*, *11*, 212.

McLaurin, KA, Cook, AK, Li, H, League, AF, Mactutus, CF, & Booze, RM (2018). Synaptic connectivity in medium spiny neurons of the nucleus accumbens: A sex-dependent mechanism underlying apathy in the HIV-1 transgenic rat. *Frontiers in Behavavioral Neuroscience, 12,* 285

Moran, L. M., Aksenov, M. Y., Booze, R. M., Webb, K. M., & Mactutus, C. F. (2012). Adolescent HIV-1 transgenic rats: evidence for dopaminergic alterations in behavior and neurochemistry revealed by methamphetamine challenge. *Current HIV research*, *10*(5), 415–424. https://doi.org/10.2174/157016212802138788

Nimmerjahn, A., Kirchhoff, F., & Helmchen, F. (2005). Resting microglial cells are highly dynamic surveillants of brain parenchyma in vivo. *Science*, *308*(5726), 1314-1318.

Ohsawa, K., Imai, Y., Sasaki, Y., & Kohsaka, S. (2004). Microglia/macrophage-specific protein Iba1 binds to fimbrin and enhances its actin-bundling activity. *Journal of neurochemistry*, *88*(4), 844-856.

Qi, Y., Yu, T., Xu, J., Wan, P., Ma, Y., Zhu, J., Li, Y., Gong, H., Luo, Q., & Zhu, D. (2019). FDISCO: Advanced solvent-based clearing method for imaging whole organs. *Science advances*, *5*(1), eaau8355.

Ramos-Vara, J. A. (2005). Technical aspects of immunohistochemistry. *Veterinary pathology*, *42*(4), 405-426.

Ramos-Vara, J. A., & Miller M. A. (2014). When tissue antigens and antibodies get along: revisiting the technical aspects of immunohistochemistry--the red, brown, and blue technique. *Veterinary Pathology*, *51*(1), 42-87.

Ransohoff, R. M., & Cardona, A. E. (2010). The myeloid cells of the central nervous system parenchyma. *Nature*, *468*(7321), 253-262.

Reid, W., Sadowska, M., Denaro, F., Rao, S., Foulke, J., Hayes, N., Jones, O., Doodnauth, D., Davis, H., Sill, A., O'Driscoll, P., Huso, D., Fouts, T., Lewis, G., Hill, M., Karmin-Lewis, R., Wei, C., Ray, P., Gallo, R. C., … O'Driscoll, P. (2001). An HIV-1 transgenic rat that develops HIV-related pathology and immunologic dysfunction. *Proceedings of the National Academy of Sciences*, *98*(16), 9271-9276.

Renier, N., Adams, E. L., Kirst, C., Wu, Z., Azevedo, R., Kohl, J., Autry, A. E., Kadiri, L., Venkataraju, K. U., Zhou, Y., Wang, V. X., Tang, C. Y., Olsen, O., Dulac, C., Osten, P., & Tessier-Lavigne, M. (2016). Mapping of brain activity by automated volume analysis of immediate early genes. *Cell*, *165*(7), 1789-1802.

Renier, N., Wu, Z., Simon, D. J., Yang, J., Ariel, P., & Tessier-Lavigne, M. (2014). iDISCO: a simple, rapid method to immunolabel large tissue samples for volume imaging. *Cell*, *159*(4), 896-910.

Richardson, D. S., & Lichtman, J. W. (2015). Clarifying Tissue Clearing. *Cell*, *162*(2), 246–257. https://doi.org/10.1016/j.cell.2015.06.067

Rocha, M. D., Düring, D. N., Bethge, P., Voigt, F. F., Hildebrand, S., Helmchen, F., Pfeifer, A., Hahnloser, R., & Gahr, M. (2019). Tissue Clearing and Light Sheet Microscopy: Imaging the Unsectioned Adult Zebra Finch Brain at Cellular Resolution. *Frontiers in neuroanatomy*, *13*, 13. https://doi.org/10.3389/fnana.2019.00013

Roostalu, U., Zois, N. E., Pedersen, P. G., Pedersen, T. X., Vrang, N., & Hecksher Sorensen, J. (2019). 3D Light Sheet Imaging of Left Anterior Descending Artery Ligation-Induced Myocardial Infarction in Mice. *Circulation*, *140*(Suppl_1), A13303-A13303.

Rowson, S. A., Harrell, C. S., Bekhbat, M., Gangavelli, A., Wu, M. J., Kelly, S. D., Reddy, R., & Neigh, G. N. (2016). Neuroinflammation and Behavior in HIV-1 Transgenic Rats Exposed to Chronic Adolescent Stress. *Frontiers in psychiatry*, *7*, 102. https://doi.org/10.3389/fpsyt.2016.00102

Royal III, W., Cherner, M., Burdo, T. H., Umlauf, A., Letendre, S. L., Jumare, J., ... & Okwuasaba, K. (2016). Associations between cognition, gender and monocyte activation among HIV infected individuals in Nigeria. *PloS one*, *11*(2).

Sengupta P. (2013). The laboratory rat: relating its age with human's. *International journal of preventive medicine*, *4*(6), 624–630.

Sengupta, S., & Siliciano, R. F. (2018). Targeting the Latent Reservoir for HIV-1. *Immunity*, *48*(5), 872–895. https://doi.org/10.1016/j.immuni.2018.04.030

Silvers, J. M., Aksenov, M. Y., Aksenova, M. V., Beckley, J., Olton, P., Mactutus, C. F., & Booze, R. M. (2006). Dopaminergic marker proteins in the substantia nigra of human immunodeficiency virus type 1-infected brains. *Journal of neurovirology*, *12*(2), 140–145. https://doi.org/10.1080/13550280600724319

Silvestri, L., Costantini, I., Sacconi, L., & Pavone, F. S. (2016). Clearing of fixed tissue: a review from a microscopist's perspective. *Journal of biomedical optics*, *21*(8), 081205.

Smyth, R. P., Davenport, M. P., & Mak, J. (2012). The origin of genetic diversity in HIV-1. *Virus research*, *169*(2), 415-429.

Sundermann, E. E., Heaton, R. K., Pasipanodya, E., Moore, R. C., Paolillo, E. W., Rubin, L. H., Ellis, R., Moore, D. J., & HNRP Group (2018). Sex differences in HIV-associated cognitive impairment. *AIDS (London, England)*, *32*(18), 2719–2726. https://doi.org/10.1097/QAD.0000000000002012

Susaki, E. A., Tainaka, K., Perrin, D., Kishino, F., Tawara, T., Watanabe, T. M., Yokoyama, C., Onoe, H., Eguchi, M., Yamaguchi, S., Abe, T., Kiyonari, H., Shimizu, Y., Miyawaki, A., Yokota, H., & Ueda, H.R. (2014). Whole-brain imaging with single-cell resolution using chemical cocktails and computational analysis. *Cell*, *157*(3), 726-739.

Ueda, H. R., Ertürk, A., Chung, K., Gradinaru, V., Chédotal, A., Tomancak, P., & Keller, P. J. (2020). Tissue clearing and its applications in neuroscience. *Nature Reviews Neuroscience*, 1-19.

UNAIDS. *19.6 Million Girls and Women Living with HIV*. Available online at, https://www.unaids.org/sites/default/files/girls-and-women-living-with-HIV_en.pdf. (2019).

UNAIDS. *Fact Sheet*. Available online at, http://www.unaids.org/sites/default/files/media_asset/UNAIDS_FactSheet_en.pdf. (2019).

Vera, J. H., Guo, Q., Cole, J. H., Boasso, A., Greathead, L., Kelleher, P., Rabiner, E. A., Kalk, N., Bishop, C., Gunn, R. N., Matthews, P. M., & Winston, A. (2016). Neuroinflammation in treated HIV-positive individuals: A TSPO PET

study. *Neurology*, *86*(15), 1425–1432. https://doi.org/10.1212/WNL.0000000000002485

Vigorito, M., Connaghan, K. P., & Chang, S. L. (2015). The HIV-1 transgenic rat model of neuroHIV. *Brain, behavior, and immunity*, *48*, 336-349.

Wallace, D. R., Dodson, S., Nath, A., & Booze, R. M. (2006). Estrogen attenuates gp120- and tat1–72-induced oxidative stress and prevents loss of dopamine transporter function. *Synapse*, *59*(1), 51-60.

Webb, K. M., Aksenov, M. Y., Mactutus, C. F., & Booze, R. M. (2010). Evidence for developmental dopaminergic alterations in the human immunodeficiency virus-1 transgenic rat. *Journal of neurovirology*, *16*(2), 168–173. https://doi.org/10.3109/13550281003690177

West, Mark J (university Of Aarhus, Denmark). (2012). *Basic stereology for biologists and neuroscientists*. Scion Publishing Ltd.

Zigmond, M. J., Acheson, A. L., Stachowiak, M. K., & Strickerm, E. M. (1984). Neurochemical compensation after nigrostriatal bundle injury in an animal model of preclinical parkinsonism. *Archives of neurology*, *41*(8), 856-861.

APPENDIX A

SOLUTION RECIPES

PTx.2 (1L)
- 900mL H2O
- 100mL PBS 10X
- 2mL TritonX-100

PTwH (1L)
- 900mL H2O
- 100mL PBS 10X
- 2mL Tween-20
- 1mL of 10mg/mL Heparin stock solution

Permeabilization Solution (500mL)
- 400mL PTx.2
- 11.5g of Glycine
- 100mL of DMSO

Blocking Solution (50mL)
- 42mL PTx.2
- 3mL of Goat Serum
- 5mL of DMSO

Tyrosine Hydroxylase Primary
- 93% PTwH
- 5% DMSO
- 3% Goat Serum
- 1:100 Tyrosine hydroxylase primary antibody

Iba1 Primary
- 93% PTwH
- 5% DMSO
- 3% Goat Serum
- 1:200 Iba1 primary antibody

Secondary Antibody (for both TH and Iba1)
- 97% PTwH
- 3% Goat Serum
- 1:100 Anti-rabbit secondary antibody

APPENDIX B

SUPPLIER INFORMATION

Table B.1: Supplier information and catalog numbers.

Name of Material/Equipment	Company	Catalog Number
DBE	Sigma-Aldrich	108014-1KG
DCM	Sigma-Aldrich	270997-100mL
DMSO	Sigma-Aldrich	472301-1L
Glycine	Fisher Chemical	G46-500
Goat anti-rabbit Alexa Fluor Plus 647	Invitrogen	A32733
Goat serum	Sigma Life Science	G9023-10mL
Heparin	Acros Organics	41121-0010
Iba1 primary antibody	FUJIFILM Wako	019-19741
Kwik-sil epoxy	VWR	MSPP-KWIK-SIL
Methanol	Sigma-Aldrich	34860-1l-R
PBS	Fisher Bioreagents	BP2944-100
Perfusion pump	VWR	70730-062
PFA	Sigma-Aldrich	158127-3KG
TritonX-100	Fisher Bioreagents	BP151-500
Tween-20	Fisher Bioreagents	BP337-500
Tyrosine hydroxylase primary antibody	Millipore Sigma	AB152